A metamorphic origin for Europa's ocean

Mohit Melwani Daswani[1], Steven D. Vance[1], Matthew J. Mayne[2], Christopher R. Glein[3]

[1]Jet Propulsion Laboratory, California Institute of Technology, Pasadena, CA, USA
[2]Department of Earth Sciences, Stellenbosch University, RSA
[3]Space Science and Engineering Division, Southwest Research Institute, San Antonio, TX, USA

Key Points:

- Devolatilization of early Europa's rocky interior may have generated a mildly acidic ocean
- Heating drove outgassing of up to 1–270 bar CO_2, perhaps as an early atmosphere since lost, or captured as a large clathrate reservoir
- Calcium, sulfate and carbonate salts precipitate at the seafloor, while chloride is abundant nearer the ice shell

Corresponding author: M. Melwani Daswani, mohit.melwani.daswani@jpl.caltech.edu

Abstract

Europa likely contains an iron-rich metal core. For it to have formed, temperatures within Europa reached $\gtrsim$1250 K. At that temperature, accreted chondritic minerals—e.g., carbonates and phyllosilicates—would partially devolatilize. Here, we compute the amounts and compositions of exsolved volatiles. We find that volatiles released from the interior would have carried solutes, redox-sensitive species, and could have generated a carbonic ocean in excess of Europa's present-day hydrosphere, and potentially an early CO_2 atmosphere. No late delivery of cometary water was necessary. Contrasting with prior work, CO_2 could be the most abundant solute in the ocean, followed by Ca^{2+}, ${SO_4}^{2-}$, and ${HCO_3}^{-}$. However, gypsum precipitation going from the seafloor to the ice shell decreases the dissolved S/Cl ratio, such that Cl>S at the shallowest depths, consistent with recently inferred endogenous chlorides at Europa's surface. Gypsum would form a 3–10 km thick sedimentary layer at the seafloor.

1 Introduction

Key to understanding the past and present habitability of Jupiter's moon Europa is its composition and evolution. Europa hosts a $\gtrsim$ 100 km deep liquid water ocean beneath its 3–30 km ice shell (e.g., Schubert et al., 2009). Water, solutes and possible oxidants needed to carry out metabolic processes (Gaidos et al., 1999; Hand et al., 2007) in Europa's ocean were delivered through some combination of Europa's accreted materials, release by chemical reactions, and subsequently by meteoritic or Io-genic influx.

Surface spectra were initially interpreted as hydrated surface salts from a sulfate-rich ocean (McCord et al., 1998), consistent with models of brine evolution in CI chondrite bodies (Kargel, 1991; Kargel et al., 2000; Zolotov & Shock, 2001). These models propose that Europa's ocean evolved from a reduced NaCl-dominated composition to a more oxidized Mg-sulfate ocean as a result of: 1) thermodynamic equilibrium (including by hydrothermal activity) between the ocean and silicate interior, while reduced volatiles H_2 and CH_4 produced by water-rock interaction escaped (Zolotov & Shock, 2001, 2004; Zolotov & Kargel, 2009); and/or 2) large fluxes of surface-derived oxidants delivered into the ocean through overturning of the icy lithosphere (Hand et al., 2007; Pasek & Greenberg, 2012). Recently, however, a sulfate-rich ocean has been challenged because the interpretation of hydrated sulfate salts on the surface as an oceanic signature is not apparently consistent with more recent spectroscopic observations. These observations favor instead chloride salts on the most geologically disrupted surfaces; surface sulfate salts and hydrated sulfuric acid are interpreted as radiolytic end-products (Brown & Hand, 2013; Ligier et al., 2016; Trumbo et al., 2019, 2017; Fischer et al., 2016, but cf. Dalton et al., 2013). Alternatively, the ocean may have remained reduced and sulfidic if H_2 and CH_4 escape to space was limited (McKinnon & Zolensky, 2003).

Here, we use geochemical and petrologic models to assess whether planetary-scale thermal processes were responsible for the build-up of Europa's ocean, and whether thermal evolution of the deep interior had a significant impact on the composition of the ocean. While plausible models of Europa have been constructed without a solid iron-rich core (Table S1), Europa's high density and the inferred molten iron core in neighboring Ganymede (Bland et al., 2008) strongly suggest a high-temperature history for Europa's interior (e.g., Greeley et al., 2004; Tobie et al., 2003, 2005) consistent with the formation of an iron-rich core (Anderson et al., 1998; Schubert et al., 2009; Moore & Hussmann, 2009). The decay of short-lived radionuclides in the accreting material could have heated the silicate interior sufficiently for partial melting to separate silicate and metal (c.f. Barr & Canup, 2008), or to at least expel volatiles, as occurred during the thermal metamorphism of some chondrites (e.g., Huss et al., 2006). Additionally, tidal dissipation during Europa's orbital evolution may haveaffected early heating and differentiation of the

interior at a level comparable to radiogenic heating, but disentangling the influence of tidal dissipation from other early sources of heat is difficult (Hussmann & Spohn, 2004).

If Europa has an Fe-rich core, then a fraction of the deep interior was heated at least to the Fe ± S eutectic temperature during differentiation. Accordingly, we hypothesize that prograde metamorphism (i.e., metamorphic changes caused by increasing temperature) and associated chemical reactions in the deep interior were the driving forces behind the ocean's formation and its composition. Based on this prograde assumption for Europa's evolution we: 1) establish a starting bulk composition of Europa immediately after accretion using an accretion model and compositional endmember scenarios; 2) use a Gibbs free energy minimization petrologic model to constrain a range of compositions for the changing ocean and deep interior during thermal excursions that could be caused by differentiation and/or thermal-orbital evolution (e.g., Tobie et al., 2005; Hussmann & Spohn, 2004); 3) use a chemical equilibrium model to calculate the composition of Europa's ocean after itsgeneration by metamorphic reactions; and 4) constrain the present composition and interior structure of Europa by using mass balance and a 1D interior structure model consistent with Europa's gravitational coefficients and moment of inertia (MoI).

2 Methods

A flow chart summarizing the methods below is shown in Figure S1.

2.1 Bulk composition of the accreted body

To date, accretion models have suggested that Europa's bulk water content was derived from dust, pebbles or satellitesimals composed of non-hydrated silicate, plus varying amounts of water ice as a function of the (possibly migrating) position of the circumjovian snow line towards the late stages of accretion (e.g. Lunine & Stevenson, 1982; Makalkin et al., 1999; Canup & Ward, 2002, 2009; Ronnet et al., 2017), and/or capture and impact processing (e.g. Estrada et al., 2009; Mosqueira et al., 2010; Ronnet & Johansen, 2020). Both scenarios can lead to bodies consistent with models of the density gradient in the Galilean satellites and orbital properties, but rely on the fortuitous delivery of the exact mass of water as ice to explain the present-day hydrosphere (8—12 wt. %) despite widely different sizes ($\sim 10^{-3}$-–10^{5} m radius) and water ice contents (0.571–50 wt. %; Ronnet et al., 2017; Ronnet & Johansen, 2020) of the accreting particles. A recent reappraisal of hydrodynamic escape during accretion also yields water contents and densities consistent with present day observations (Bierson & Nimmo, 2020). The alternative that we explore here is one where variable amounts of water and volatiles are already present in Europa's accreting particles, based on the compositions of the proposed silicate-rich building blocks of Europa (i.e., chondrites) according to geophysical and geochemical models (Kargel et al., 2000; Zolotov & Shock, 2001; McKinnon & Zolensky, 2003; Kuskov & Kronrod, 2005; Zolotov & Kargel, 2009), and tie the subsequent thermal evolution of the accreted body to present-day Europa's spherical structure and gravitational moment of inertia. Chondrites contain various amounts of volatiles in minerals and organics (Table S2), the thermal processing of which could yield sufficient mass to form the present-day hydrosphere and still fulfill the geophysical constraints. (A present-day hydrated silicate interior for Europa is implausible given gravity and density measurements (Anderson et al., 1998; Sohl et al., 2002; Schubert et al., 2009; Kuskov & Kronrod, 2005; Vance et al., 2018), so subsequent thermal processing, nominally *differentiation* of the body will be necessary to meet the constraints.)

The composition and water mass fraction for the initial state of Europa before differentiation (*MC-Scale*) are estimated using a Monte Carlo accretion model (`AccretR`). Additionally, we consider two endmember compositions: one in which Europa accreted

entirely from CI carbonaceous chondrites (*EM-CI*), and another in which Europa accreted from CM chondrites only (*EM-CM*).

The models are insensitive to the mineralogy of the initial pebbles/satellitesimals and whether these were in thermochemical equilibrium prior to accretion (McKinnon & Zolensky, 2003) because our calculations of the subsequent geochemical evolution of these materials depend on the bulk composition, not the mineralogy. Nevertheless, hydrous minerals in planetesimal collisions are predicted to survive without substantial dehydration (Wakita & Genda, 2019). Further details about the accretion and composition models, and an additional model exploring a hypothetical reduced CI chondrite body are shown in Text S1 and Figures S4-S5, and the initial bulk compositions are summarized in Table S3.

2.2 Ocean build-up by prograde metamorphism until the onset of core formation

To determine the mass and composition of an ocean produced during heating, devolatilization, and differentiation of the deep interior, we use the `Perple_X` Gibbs free energy minimization program, which leverages experimental and modeled thermodynamic data, including non-aqueous solvents, and the Deep Earth Water model optimized for computing aqueous fluid speciation at high pressure (e.g. Connolly, 2005, 2009; Connolly & Galvez, 2018; Pan et al., 2013). For each initial bulk composition (§2.1), we model a 0-dimensional heating pathway throughout the deep interior using `Rcrust` (Mayne et al., 2016), which provides an interface to model complex phase fractionation. We construct a 1D column spanning the radius of Europa discretized into a number of vertical cells that experience isobaric heating steps, and track the composition and mass of the equilibrium mineral-plus-volatile assemblage. At each heating step (ΔT), the Gibbs energy of the assemblage in each cell is minimized, resulting in a new equilibrium assemblage that depends on the heating step directly prior to it, but is not affected by the adjacent vertical cells.

We simulate the build-up of the ocean by imposing a limit on the fraction of volatiles retained in the assemblage for each heating step. That is, if fluids (except silicate melt, see below) are thermodynamically stable, a specified portion is irreversibly fractionated from the equilibrium assemblage of the particular cell to go into the growing ocean reservoir (Fig. 1). As a limiting case, for each bulk composition computed (§2.1) we apply our thermodynamic models with a retained-to-extracted (R/E) fluid mass ratio of 0, i.e., all fluids (including gases, liquids and their dissolved species) produced during heating are extracted from the interior. Buoyancy drives fluids upward, with transport being particularly rapid in permeable materials in the direction of maximum compressive stress (e.g. Richard et al., 2007). Long-term retention of fluids at high pressure would lead to an unstable solution that is out of hydrostatic equilibrium. Thus, the only path for free low density fluids is up. This efficient extraction of volatiles from Europa's interior is consistent with findings for the more limiting case of Titan (Leitner & Lunine, 2019) where a volatile-rich hydrosphere and atmosphere were formed endogenously (Miller et al., 2019; Néri et al., 2020) despite higher overburden pressure and gravity, and reduced tidal heating, that would more efficiently prevent their escape.

A CI chondrite Europa's bulk composition would contain water in excess of Europa's present hydrosphere (§2.1), so for *EM-CI*, we also test the effect of varying the R/E fluid mass ratio, and carry out a model with a R/E ratio of 0.1 at each heating step, i.e., at each ΔT, thermodynamic equilibrium is computed, and subsequently 1 part of fluid is retained for 10 parts of fluid extracted. For *EM-CI* we also test the effect of a constant mass of fluid present in the rocky interior by retaining 5 wt. % fluid and extracting any fluid in excess, similar to how magma chambers reach a critical size threshold prior to eruption (e.g. Townsend & Huber, 2020). (See Text S2 for model param-

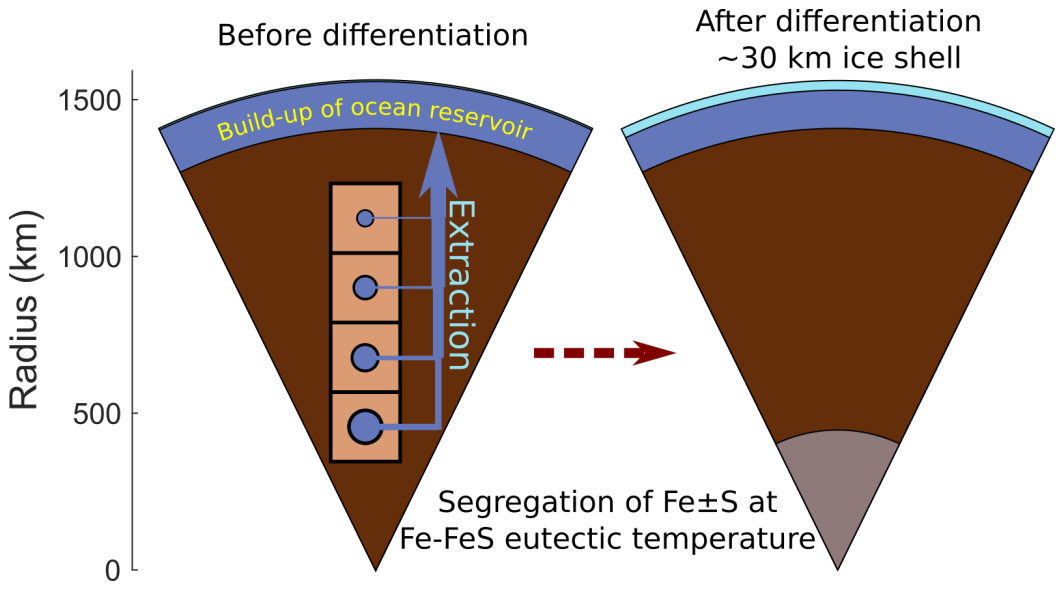

Figure 1. Schematic of the thermodynamic + extraction + structure model to simulate the build-up of Europa's ocean from exsolved volatiles. After each heating step before differentiation, Gibbs energy minimization is carried out, resulting in an equilibrium assemblage in each cell (left figure). A portion of the fluid phase(s) is then extracted according to a specified rule (see §2.2), joins the ocean reservoir, and no longer affects the chemistry of the deep interior. Fe ± S is extracted from the bulk composition from the deep interior once the interior reaches the Fe-FeS eutectic temperature (§2.3). Finally, Europa's structure is resolved (§2.4), here assuming a 30 km ice shell, requiring a temperature of 270.8 K at the ice-ocean interface.

eters and validation, and Table S4 for activity-composition modelsused.) As discussed, Europa likely contains a Fe-rich core, so the lowest maximum temperature the interior reached during prograde metamorphism is the melting temperature of the Fe-rich phase(s) that eventually formed the core (§2.3). Therefore, the resulting concentrations we report here represent a lower limit of the exsolved and extracted volatiles that formed Europa's proto-ocean. The onset of differentiation occurs at a temperature lower than the temperature of silicate melting (§2.3), hence silicate partial melting does not occur here.

2.3 Core composition

In our model we assume that prograde metamorphism proceeded at least up to the Fe-FeS eutectic temperature in order for core formation to proceed. Since this occurs at temperatures higher than volatile-releasing metamorphic reactions (see §2.2), we further assume that core formation does not sequester volatiles that would build the ocean. Our calculations are performed in the simplified Fe-S system as an initial approximation for an expected core composition, mass and density, until a future mission can constrain the deep interior composition of Europa from its seismic properties and improved gravity data. For further details on assumptions taken for modelled temperatures and the chemical system considered see Text S3.

2.4 Post-differentiation structure, mineralogy and geochemistry

We obtain our final predictions for Europa's interior structure after the formation of the ocean and differentiation using `PlanetProfile`, a program for constructing 1D

planetary structure models, in which the self-consistent gridded thermodynamic properties from `Perple_X` and `Rcrust` are used as inputs (Vance et al., 2018). To construct the inputs, we first use `Rcrust` to perform isobaric heating simulations as described in §2.2 and Figure 1 to obtain the thermodynamic properties. We then remove the appropriate Fe ± S mass from the silicate layer for each model Europa to form a core with 24 mass % sulfur (the minimum amount of sulfur in melt at the Fe-FeS eutectic within Europa, see §2.3) for *EM-CI*, *EM-CM* and *MC-Scale* after fluid extraction up to the Fe-FeS eutectic temperature (§2.2). Finally, we fold the separate silicate layer and Fe ± S core (§2.3) thermodynamic properties into `PlanetProfile` and obtain structures consistent with Europa's radius, density and MoI. Text S4 describes inputs and modifications to `PlanetProfile` for this work. The results form a baseline against which spacecraft observations may be compared to elucidate the effects of ∼ 4.5 Gyr of orbital-geologic history.

2.5 Ocean column composition

We use the bulk extracted ocean compositions and masses (§2.2) as inputs into geochemical model `CHIM-XPT` (Reed, 1998) to compute ocean depth dependent mineral-aqueous solution-gas equilibria using the self-consistent thermodynamic database SOLTHERM, which includes thermodynamic properties of water and equilibrium constants up to 0.5 GPa. We carry out a 1D `CHIM-XPT` model for the bulk fluids extracted by prograde metamorphism of *EM-CI*, *EM-CM*, and *MC-Scale* (§2.2), varying the pressure from the seafloor (200 MPa; Vance et al., 2018) up to a hypothetical ice-free surface. This way, we quantify gas saturation and mineral precipitation out of the primordial ocean (i.e., fractionation), and the effects on the water column's composition, pH and redox potential. Further details about `CHIM-XPT` and validation of the model are found in Text S2.

3 Results and discussion

Prograde metamorphism up to the Fe-FeS eutectic temperature has the effect of dehydrating, dehydroxylating, decarbonizing and desulfurizing the deep interior, irreversibly changing the mineralogy (e.g., Glein et al., 2018). The main volatile-releasing generalized reactions are:

$$\underset{\text{antigorite}}{Mg_3Si_2O_5(OH)_4} \longrightarrow \underset{\text{forsterite}}{Mg_2SiO_4} + \underset{\text{(clino)enstatite}}{MgSiO_3} + 2\,H_2O \tag{1}$$

$$\underset{\text{antigorite}}{Mg_3Si_2O_5(OH)_4} + \underset{\text{magnesite}}{MgCO_3} \longrightarrow 2\,\underset{\text{forsterite}}{Mg_2SiO_4} + 2\,H_2O + CO_2 \tag{2}$$

Large amounts of volatiles are released at low temperature (< 300 K): the starting rock compositions (namely volatile-rich carbonaceous chondrites) are thermally unequilibrated, so the thermodynamic model predicts that excess volatiles (mainly water and CH_4) and dissolved solutes are unbound from minerals and organics. At moderate temperatures (300–600 K), only small amounts of fluid are released because lizardite, antigorite, chlorite and magnesite are stable; these are phyllosilicate or carbonate minerals with structurally bound water and OH^-, or CO_3^{2-}. At $\gtrsim$ 650 K, antigorite and magnesite break down, releasing H_2O and CO_2. Higher pressure stabilizes magnesite and antigorite, whereas lower pressure favors their breakdown at that temperature. Analogous volatile-releasing reactions occur presently in Earth's subducting oceanic plates, for example, which experience dewatering and decarbonization with increasing pressure and temperature (e.g., Manthilake et al., 2016; Gorce et al., 2019). Further details about the pressures and temperatures of the reactions and the changing mineralogy along the prograde metamorphic path are found in Text S5 and Figures S12–S13.

3.1 Extracted fluid compositions and ocean masses

Prograde metamorphism of the *EM-CI* and *EM-CM* initial compositions supplies a fluid mass that exceeds the present ∼ 10 wt. % hydrosphere for all tested R/E ratios. The *MC-Scale* composition however, is unable to supply sufficient fluid mass, despite a R/E ratio = 0, since the maximal water content of this composition (3.5 ± 0.6 wt %, assuming all H is in H_2O) falls short of Europa's present hydrosphere mass, indicating that additional water was co-accreted or delivered if Europa formed from the materials nearest to Jupiter ∼ 4.5 Ga according to the MC accretion model (§2.1).

The pattern of volatile release at different pressures and temperatures is broadly similar for all prograde metamorphism models of the initial compositions tested. We focus on solutes and solvents from *EM-CM* shown in Fig. 2, and include additional subtleties of the exsolved fluid compositions in Text S5, Table S5 and Figures S6–S11. In all cases, the most significant contributors to the ocean reservoir mass are oxygen and hydrogen, as water (e.g., Fig. 2). Carbon is the third most abundant element comprising the ocean reservoir of the *EM-CI* and *EM-CM* models, particularly at relatively high temperatures where CO_2 becomes a major component, and acts as the solvent, in the fluid phase (Fig. 2) as a result of carbonate destabilization (see also §3.3). However, while carbon, hydrogen, oxygen, sulfur and calcium abundances in the exsolved ocean reservoirs of *EM-CI* and *EM-CM* are comparable, the total mass of silicon, sodium, magnesium, chlorine, potassium and aluminum extracted from *EM-CM* is significantly higher, and only the extracted mass of iron is lower after prograde metamorphism of *EM-CM* compared to *EM-CI*. For *MC-Scale*, the most abundant solutes in the extracted ocean are calcium and sulfur, especially exsolved at <650 K and >6 GPa in the form of $CaSO_4$, although some calcium is present as $CaCl_2$.

3.2 Composition of the ocean column, precipitated minerals and exsolved gases

Distinct ocean compositions from seafloor to surface (Fig. 3) result from isothermal 1D decompression `CHIM-XPT` models equilibrating the bulk compositions of the extracted fluids for *EM-CI*, *EM-CM* and *MC-Scale* (§3.1). In all cases, gypsum ($CaSO_4$) saturates and precipitates as pressure decreases. Additionally, for *EM-CM*, dolomite is stable throughout the water column, while for *MC-Scale*, dolomite is stable at < 30 MPa, which may correspond to a depth within the present ice shell (Fig. 3). (Since prograde metamorphism of the *MC-Scale* composition did not yield a sufficiently massive hydrosphere (§3.1), we consider the effects of compensating the difference with late delivery of cometary material in Text S7 and Fig. S15.)

Gypsum precipitation throughout the water column steadily decreases the S/Cl molar ratio with decreasing depth in all cases, such that the total concentrations of chlorine and sulfur become comparable ($\Sigma Cl \approx \Sigma S$) at shallow depths for *EM-CI* and *EM-CM* (Fig. 3), and chlorine exceeds sulfur at $\lesssim$ 124 MPa for *EM-CI*. Similarly, the dissolved calcium concentration decreases as a result of gypsum precipitation, decreasing the Ca/Mg molar ratio with decreasing depth in all models. No Na- or K-bearing minerals saturate, so the Na/K molar ratio remains constant at all depths. In the limiting assumption of zero porosity, the globally averaged thickness of all mineral precipitates at Europa's seafloor is 2.7–9.5 km (Table 1).

The combined mass of gases (particularly CO_2) that would boil out of the ocean at low pressure (i.e., at < 20 MPa for a hypothetical non-ice covered surface) is comparable to the mass of precipitated minerals (Fig. 3 and Table 1). The massive outgassing of volatiles (0.06–1.33 % Europa's mass; Table 1) may have led to an early CO_2-rich atmosphere of considerable thickness, on the order of 1–27 MPa for the mass of exsolved gases calculated if they were released all at once. (We note that 5–25 MPa of H_2O and in excess of 1–5.5 MPa of CO_2 are calculated to have been lost from Mars < 12 Myr

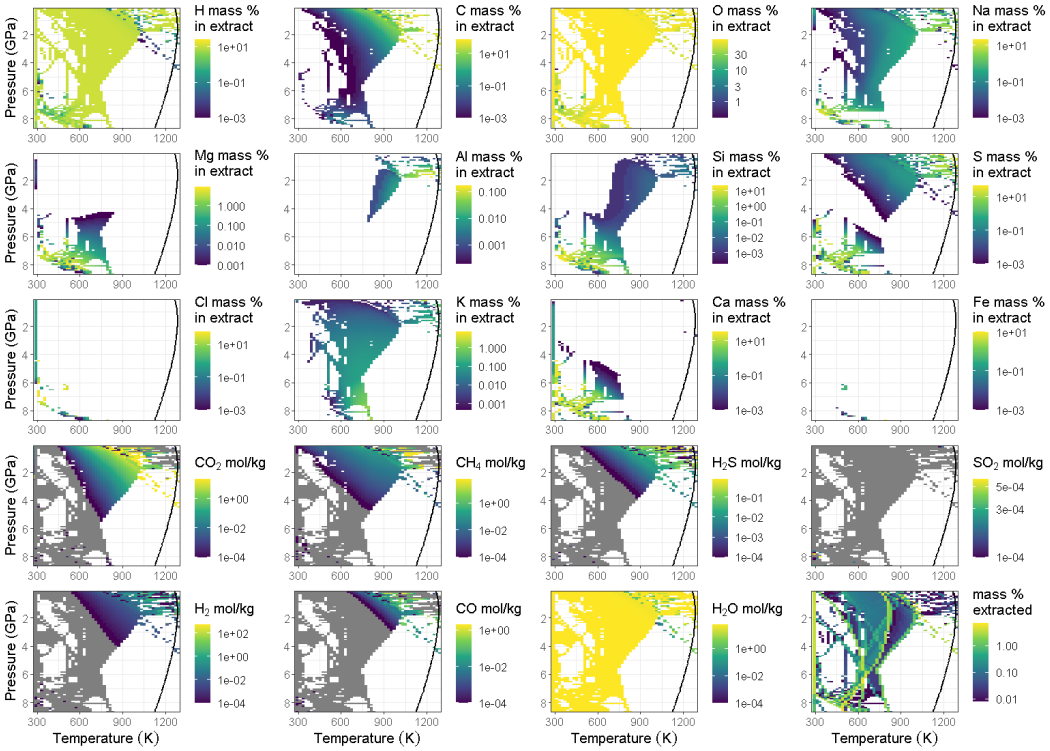

Figure 2. Composition of the fluid extracted from the deep interior at different pressures with increasing temperature for the *EM-CM* R/E=0 model. Solid curves show the Fe-FeS eutectic temperature. Integrating up to the eutectic yields the total amounts exsolved from the deep interior. Blank areas signify that no fluids containing the specific element shown in the plot were extracted at those pressures and temperatures. Rows 1–3: elemental abundance of the extracted fluid (solvents and solutes). Rows 4–5: molecular solvent moles per kilogram of extracted fluid. Grey areas in the solvent plots signify that fluids were extracted at those pressures and temperatures, but did not contain the specific solvent shown in the plot. Bottom-right plot: total (solvent + solute) extracted mass. For corresponding figures of the broadly similar patterns of exsolution in the *EM-CI* and *MC-Scale* models, see Figures S7–S10

.

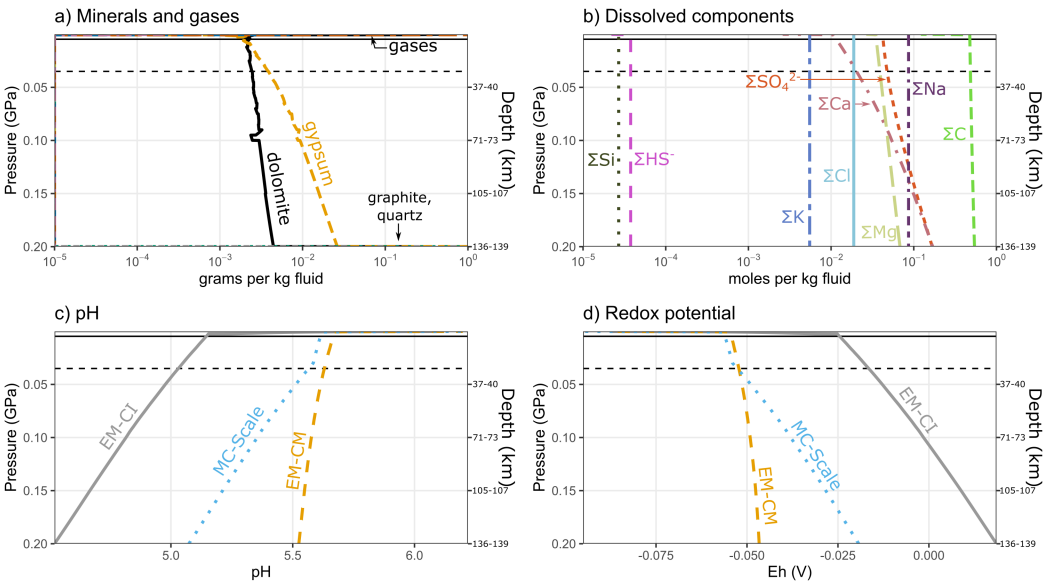

Figure 3. Ocean column compositions from the seafloor to the surface, for *EM-CM*. Solid and horizontal lines show the pressure at the base of a current 5 km and 30 km ice shell respectively (see §3.3). a) Minerals precipitated and gases exsolved with decreasing depth in the water column. b) Total dissolved components in the water column. Dissolved components shown here are the sum of those particular components distributed among all species in solution. For example, component ΣC represents the sum of carbon in aqueous HCO_3^-, CH_4, CO_2, and organics, among other species. Concentrations $< 10^{-5}$ mol/kg not shown. c) pH, and d) redox potential of the ocean column for the R/E = 0 models of *EM-CI*, *EM-CM* and *MC-Scale*.

after accretion (Erkaev et al., 2014; Odert et al., 2018). Massive primordial atmospheres have also been predicted for Triton ($\sim$ 16 MPa pCO_2; Lunine & Nolan, 1992), Titan, Ganymede and Callisto (Kuramoto & Matsui, 1994).) With such a thick atmosphere, greenhouse trapping of heat generated by insolation (Zahnle & Catling, 2017), radioactive decay or tides would likely vaporize Europa's hydrosphere, although exceedingly high rates of atmospheric escape by ionization in Jupiter's magnetosphere, or solar energetic particles and galactic cosmic rays, would have likely either prevented atmospheric build-up, or allowed recondensation of the hydrosphere.

More likely, the rate of heating (radioactive or tidal) would control the rate of exsolution from the deep interior, ocean build-up, and the subsequent mass outgassed from the ocean. Based on mass ejection rates from tentative plume detections (Roth et al., 2014; Sparks et al., 2016), plumes could output up to 7.2×10^{19}–7.2×10^{20} kg of H_2O over the lifetime of the solar system, or about 1.4–24 % of Europa's present ocean mass (Text S6). Alternatively, clathrate hydrates could trap dissolved carbon and limit CO_2 outgassing. Whether CO_2 clathrates are stable in Europa's ocean depends on the pressure and temperature, assuming sufficient CO_2 feedstock is present. For the large amounts of CO_2 produced here we predict structure I clathrates with a CO_2/H_2O molar ratio of 0.159 at 273.15 K and equilibrium pressure (1.24 MPa), with a density of 1106 kg/m^3 (see Text S6 for details). This exceeds the ocean's density, so these clathrates would sink, forming a 3.4–77 km layer on the seafloor. However, the long term stability of such a clathrate layer may be unfavorable because: 1) temperatures > 277 K preclude CO_2 clathrate stability in Europa's ocean (Text S6 and Fig. S14), and magmatic episodes are predicted at Europa's seafloor over geologic time (Běhounková et al., 2021), and 2) formation of the ice shell would further increase the salinity and density of the ocean, inhibiting the formation of clathrates or making them buoyant.

We find major differences between the ocean compositions predicted here and those presented previously. On the basis of thermodynamic equilibrium and extensive water-rock interaction between the ocean and the seafloor, Zolotov and Kargel (2009) predicted a "low pH" fluid that rapidly ($\sim 10^6$ yr) evolved to a reduced and basic primordial ocean (pH = 13–13.6) rich in H_2, Na^+, K^+, Ca^+, OH^-, and Cl^-. The escape of H_2 may have then led to a progressively oxidized, sulfate-rich ocean today. On the other hand, work by Zolotov and Shock (2001) and Kargel et al. (2000) on the low temperature aqueous differentiation, brine evolution, and freezing of the europan ocean broadly coincides with our predictions for a sulfate- and carbonate-rich ocean, although they predict that the most abundant cation in solution would be Mg^{2+} instead of Ca^{2+}. Hansen and McCord (2008) also favored a CO_2-rich ocean based on spectroscopic observations.

We also find it significant that the composition of the ocean column is depth-dependent, such that anion and cation concentrations, pH, and redox conditions close to the seafloor are not apparently reflective of the composition nearer to the surface or at the base of the ice shell. A caveat is that the results presented here do not account for homogenizing or unmixing of the ocean column's composition by advection or convection, or latitudinal changes; a comprehensive ocean circulation model (e.g. Lobo et al., 2021) would be required to place such constraints.

3.3 Consequences of fluid extraction on the silicate mantle and structure of Europa

Removal of Fe $\pm$ S from the devolatilized deep interior at the Fe-FeS eutectic (§2.3), and calculation of Europa's structure with `PlanetProfile` using the resulting core and residual silicate mantle thermodynamic properties (§2.4) yields a spherical shell structure, MoI (0.3455–0.3457) and density consistent with present-day Europa observations, assuming a $\sim$ 30 km ice shell (Fig. 1; Text S4). (Further details about the predicted

Table 1. Adjusted mass of Europa's hydrosphere after accounting for sediments predicted to precipitate on the seafloor and mass of gases exsolved at low pressure in the ocean column. *EM-CI* = endmember CI initial bulk composition, *EM-CM* = endmember CM initial bulk composition *MC-Scale* = Monte Carlo scaled initial composition, R/E = fluid retained-to-extracted mass ratio. "Thickness" = globally averaged thickness of the precipitate layer at Europa's seafloor, for a hydrosphere depth of 140 km (see §3.3). "Adjusted hydrosphere mass" = mass of exsolved volatiles from the interior (§3.1) minus the mass of minerals precipitated and gases exsolved from the water column. M_{Eur} = mass of Europa.

	EM-CI R/E = 0		*EM-CM R/E = 0*		*MC-Scale R/E = 0*	
Mineral precipitates	Concentration g/kg fluid	Mass kg	Concentration g/kg fluid	Mass kg	Concentration g/kg fluid	Mass kg
graphite	3.92	3.82×10^{19}	3.93	2.75×10^{19}	5.34	6.89×10^{18}
pyrite	0.02	2.17×10^{17}	0	0	0.26	3.35×10^{17}
quartz	2.59	2.52×10^{19}	8.51	5.96×10^{19}	1.20	1.55×10^{18}
sulfur	0.78	7.63×10^{18}	0	0	0	0
gypsum	50.08	4.89×10^{20}	34.46	2.41×10^{20}	117.09	1.51×10^{20}
dolomite	3.28	3.20×10^{19}	7.84	5.49×10^{19}	2.86	3.68×10^{18}
	Mean density kg/m^3	Thickness km	Mean density kg/m^3	Thickness km	Mean density kg/m^3	Thickness km
Total precipitates	2305[a]	9.5[a]	2413	6.2	2300[a]	2.7[a]
	EM-CI R/E = 0		*EM-CM R/E = 0*		*MC-Scale R/E = 0*	
Gases exsolved	Concentration g/kg fluid	Mass kg	Concentration g/kg fluid	Mass kg	Concentration g/kg fluid	Mass kg
H_2O gas	2.90×10^{-2}	2.83×10^{17}	1.81×10^{-2}	1.27×10^{17}	2.06×10^{-2}	2.66×10^{16}
CO_2 gas	65.58	6.40×10^{20}	14.86	1.04×10^{20}	20.53	2.65×10^{19}
CH_4 gas	2.66×10^{-8}	2.59×10^{11}	5.90×10^{-9}	4.13×10^{10}	4.32×10^{-8}	5.57×10^{10}
H_2 gas	6.37×10^{-10}	1.34×10^{9}	3.72×10^{-10}	2.60×10^{9}	6.50×10^{-10}	8.38×10^{8}
H_2S gas	1.38×10^{-3}	1.34×10^{16}	5.66×10^{-4}	3.96×10^{15}	1.89×10^{-3}	2.44×10^{15}
	Mass (kg)		Mass (kg)		Mass (kg)	
Total gases exsolved	6.40×10^{20}		1.04×10^{20}		2.65×10^{19}	
	EM-CI R/E = 0		*EM-CM R/E = 0*		*MC-Scale R/E = 0*	
	Mass kg	A_{Hyd}/M_{Eur} Mass %	Mass kg	A_{Hyd}/M_{Eur} Mass %	Mass kg	A_{Hyd}/M_{Eur} Mass %
Adjusted hydrosphere (A_{Hyd})	8.56×10^{21}	17.83	6.51×10^{21}	13.57	1.26×10^{21}	2.63

[a]Does not include dolomite precipitated, since it is not thermodynamically stable at the seafloor of *EM-CI* (see §3.2)

deep mineralogy are found in Text S5 and Figures S12–S13. Figure S16 shows the density, heat capacity, and bulk and shear moduli of resulting profiles.)

4 Concluding remarks

We find that the resulting volatile mass evolved from Europa's deep interior is consistent with, and can even exceed, the hydrosphere's present mass. The size and composition of the ocean depend on the assumed accreted composition of Europa. Different bulk compositions lead to different mineralogies in the thermodynamic model, that mediate the escape of volatiles and solutes. To elaborate:

1. Building a volatile mass equivalent to that of Europa's current hydrosphere by prograde metamorphism prior to core formation was probable if Europa accreted a disproportionately large amount of CI or CM chondrite material, water, and/or cometary material relative to the expected abundance of these materials at Jupiter's location in the early Solar System (c.f. Desch et al., 2018). Other known chondritic materials have insufficient volatile mass extractable by metamorphism to account for Europa's present hydrosphere mass (§2.1 & §3.1).
2. Europa's ocean, if derived from thermal evolution of the interior as shown here, was carbon and sulfur-rich (§3.1). If thermal excursions in the interior (from radioactive decay and tidal dissipation) were unimportant since differentiation, geochemical equilibrium models predict that the ocean would remain CO_2, carbonate and $CaSO_4$-rich (§3.2). However, pressure has a first order effect on the ocean's composition: decreasing pressure precipitates gypsum, removing calcium and sulfur from solution, thereby increasing the relative concentration of chlorine further up the water column, such that Cl > S at $\lesssim$ 10 MPa. Thickening of the ice shell preferentially freezes in SO_4^{2-}, rejecting and concentrating Cl at the base of the ice shell in time (Marion et al., 2005), leaving the relative concentration of ${SO_4}^{2-}$ unchanged at depth.
3. While the volatile mass in the initially accreted bulk body was high (§3.1), the deep interior must be relatively volatile-free at present to meet the MoI and density constraints (§3.3). Therefore, prograde metamorphism and fluid migration into the hydrosphere was necessarily efficient in order to remove volatile mass from the interior. Volatile loss from the rocky interior in excess of the present hydrosphere mass can be accommodated by early loss to space, especially because of the high pCO_2 outgassed. Alternatively, a large portion of volatiles (particularly CO_2) would be retained in clathrates, and their periodic destabilization by tidal heating may provide oxidants and buoyant pressure at the ice-ocean interface. We rule out complete ocean freeze-out enabled by the thermal blanketing effect of a stable seafloor clathrate layer: even if a thick clathrate layer is stable at the seafloor over geologic time, $\lesssim$ 80 km thick high pressure ice layers at Ganymede and Titan with heat fluxes $>$ 6 mW/m^2 from the silicate interior are able to maintain a liquid ocean (Kalousová & Sotin, 2020). Melt and heat transport from the bottom of the clathrate layer to the ocean would occur either through hot plume conduits or solid state convection (Choblet et al., 2017; Kalousová & Sotin, 2020).
4. The CO_2-rich ocean delivered by metamorphism may facilitate life's emergence by contributing to the generation of a proton gradient between acidic ocean water and alkaline hydrothermal fluids (Camprubí et al., 2019), if the latter are present in Europa.

While these updated models are enabled by modern computational thermodynamics and data, we expect that further work will refine these results prior to the arrival of the *JUICE* and *Europa Clipper* missions in the coming decade. In particular, 4.5 Gyr of tidally-mediated magmatism may have continued to modify the deep interior, possibly driving solid-state mantle convection, volcanism, and volatile element redistribution

and loss (Běhounková et al., 2021). The oxidized ocean may have reduced in time with hydrogen generated by serpentinization enabled by thermal cracking (Vance et al., 2016), but better constraints on the conditions of fracture formation and propagation are required (Klimczak et al., 2019). Further improvements to the thermodynamic data of high pressure H_2O-CO_2 phases (Abramson et al., 2018) and their integration with thermodynamic models (e.g., `Perple_X`) are also needed to assess the build-up of the ocean: the stability of such phases can be the factor dictating whether an ocean world will be habitable (Marounina & Rogers, 2020). Finally, we have also made the simplifying assumption that fluid percolation from depth was efficient. A coupled tidal-thermodynamic-geodynamic model would more accurately determine fluid retained-to-extracted ratios.

Data Availability Statement

All data are available though Zenodo (doi to be generated prior to publication). `AccretR` is available through Melwani Daswani (2020). `PlanetProfile` is available through Vance, Styczinski, Melwani Daswani, and Vega (2020). `Rcrust` is available through Mayne et al. (2016) and `https://tinyurl.com/rcrust`.

Acknowledgments

MMD thanks Jinping Hu, Paul Byrne, Orenthal Tucker, Evan Carnahan and the Origins and Habitability Laboratory (JPL) for discussions, Saikiran Tharimena for codes, Hauke Hussmann for tidal dissipation data, and James Connolly for help with the `Perple_X` code. We thank JPL research interns Marika Leitner and Garret Levine for early contributions to this work. This work was supported by NASA through the Europa Clipper Project to MMD, SV and CRG, and NASA grant NNH18ZDA001N-HW:Habitable Worlds awarded to MMD and SV. A part of this research was carried out at the Jet Propulsion Laboratory, California Institute of Technology, under a contract with the National Aeronautics and Space Administration (80NM0018D0004).

References

Abramson, E. H., Bollengier, O., Brown, J. M., Journaux, B., Kaminsky, W., & Pakhomova, A. (2018, September). Carbonic acid monohydrate. *American Mineralogist*, *103*(9), 1468–1472. Retrieved 2020-07-22, from `https://doi.org/10.2138/am-2018-6554` doi: 10.2138/am-2018-6554

Anderson, J. D., Schubert, G., Jacobson, R. A., Lau, E. L., Moore, W. B., & Sjogren, W. L. (1998). Europa's differentiated internal structure: Inferences from four Galileo encounters. *Science*, *281*(5385), 2019–2022. Retrieved from `http://science.sciencemag.org/content/281/5385/2019` doi: 10.1126/science.281.5385.2019

Barr, A. C., & Canup, R. M. (2008). Constraints on gas giant satellite formation from the interior states of partially differentiated satellites. *Icarus*, *198*(1), 163 - 177. Retrieved from `http://www.sciencedirect.com/science/article/pii/S0019103508002595` doi: https://doi.org/10.1016/j.icarus.2008.07.004

Bierson, C. J., & Nimmo, F. (2020, July). Explaining the Galilean Satellites' Density Gradient by Hydrodynamic Escape. *The Astrophysical Journal*, *897*(2), L43. Retrieved from `http://dx.doi.org/10.3847/2041-8213/aba11a` (Publisher: American Astronomical Society) doi: 10.3847/2041-8213/aba11a

Bland, M. T., Showman, A. P., & Tobie, G. (2008, December). The production of Ganymede's magnetic field. *Icarus*, *198*(2), 384–399. Retrieved from `http://www.sciencedirect.com/science/article/pii/S0019103508002807` doi: 10.1016/j.icarus.2008.07.011

Brown, M. E., & Hand, K. P. (2013). Salts and radiation products on the surface

of Europa. *The Astronomical Journal*, *145*(4), 110. Retrieved from http://dx.doi.org/10.1088/0004-6256/145/4/110 doi: 10.1088/0004-6256/145/4/110

Běhounková, M., Tobie, G., Choblet, G., Kervazo, M., Melwani Daswani, M., Dumoulin, C., & Vance, S. D. (2021, February). Tidally Induced Magmatic Pulses on the Oceanic Floor of Jupiter's Moon Europa. *Geophysical Research Letters*, *48*(3), e2020GL090077. Retrieved 2021-02-05, from https://doi.org/10.1029/2020GL090077 (Publisher: John Wiley & Sons, Ltd) doi: 10.1029/2020GL090077

Camprubí, E., de Leeuw, J. W., House, C. H., Raulin, F., Russell, M. J., Spang, A., ... Westall, F. (2019, December). The Emergence of Life. *Space Science Reviews*, *215*(8), 56. Retrieved from https://doi.org/10.1007/s11214-019-0624-8 doi: 10.1007/s11214-019-0624-8

Canup, R. M., & Ward, W. R. (2002, December). Formation of the Galilean Satellites: Conditions of Accretion. *The Astronomical Journal*, *124*(6), 3404–3423. Retrieved from http://dx.doi.org/10.1086/344684 doi: 10.1086/344684

Canup, R. M., & Ward, W. R. (2009). Origin of Europa and the Galilean satellites. In R. T. Pappalardo, W. B. McKinnon, & K. Khurana (Eds.), *Europa* (pp. 59–83). Tucson, AZ: University of Arizona Press.

Choblet, G., Tobie, G., Sotin, C., Kalousová, K., & Grasset, O. (2017, March). Heat transport in the high-pressure ice mantle of large icy moons. *Icarus*, *285*, 252–262. Retrieved from http://www.sciencedirect.com/science/article/pii/S0019103516302524 doi: 10.1016/j.icarus.2016.12.002

Connolly, J. A. D. (2005). Computation of phase equilibria by linear programming: A tool for geodynamic modeling and its application to subduction zone decarbonation. *Earth and Planetary Science Letters*, *236*(1-2), 524–541. Retrieved 2018-08-08, from http://linkinghub.elsevier.com/retrieve/pii/S0012821X05002839 doi: 10.1016/j.epsl.2005.04.033

Connolly, J. A. D. (2009). The geodynamic equation of state: What and how. *Geochemistry, Geophysics, Geosystems*, *10*(10). Retrieved 2018-03-22, from https://agupubs.onlinelibrary.wiley.com/doi/abs/10.1029/2009GC002540 doi: 10.1029/2009GC002540

Connolly, J. A. D., & Galvez, M. E. (2018). Electrolytic fluid speciation by Gibbs energy minimization and implications for subduction zone mass transfer. *Earth and Planetary Science Letters*, *501*, 90–102. Retrieved 2019-01-07, from https://linkinghub.elsevier.com/retrieve/pii/S0012821X18304904 doi: 10.1016/j.epsl.2018.08.024

Desch, S. J., Kalyaan, A., & Alexander, C. M. O. (2018). The Effect of Jupiter's Formation on the Distribution of Refractory Elements and Inclusions in Meteorites. *The Astrophysical Journal Supplement Series*, *238*(1), 11. Retrieved from http://stacks.iop.org/0067-0049/238/i=1/a=11

Erkaev, N., Lammer, H., Elkins-Tanton, L., Stökl, A., Odert, P., Marcq, E., ... Güdel, M. (2014, August). Escape of the martian protoatmosphere and initial water inventory. *Planetary evolution and life*, *98*, 106–119. Retrieved from http://www.sciencedirect.com/science/article/pii/S0032063313002353 doi: 10.1016/j.pss.2013.09.008

Estrada, P. R., Mosqueira, I., Lissauer, J. J., D'Angelo, G., & Cruikshank, D. (2009). Formation of Jupiter and conditions for accretion of the Galilean satellites. In R. T. Pappalardo, W. B. McKinnon, & K. Khurana (Eds.), *Europa* (pp. 27–58). Tucson, AZ: University of Arizona Press.

Fischer, P. D., Brown, M. E., Trumbo, S. K., & Hand, K. P. (2016). Spatially resolved spectroscopy of Europa's large-scale compositional units at 3–4 μm with Keck NIRSPEC. *The Astronomical Journal*, *153*(1), 13. Retrieved from http://dx.doi.org/10.3847/1538-3881/153/1/13 doi: 10.3847/1538-3881/153/1/13

Gaidos, E. J., Nealson, K. H., & Kirschvink, J. L. (1999, June). Life in Ice-Covered Oceans. *Science*, *284*(5420), 1631. Retrieved from http://science.sciencemag.org/content/284/5420/1631.abstract doi: 10.1126/science.284.5420.1631

Glein, C. R., Postberg, F., & Vance, S. D. (2018). The Geochemistry of Enceladus: Composition and Controls. In *Enceladus and the Icy Moons of Saturn.* The University of Arizona Press. Retrieved 2020-07-30, from https://uapress.arizona.edu/book/enceladus-and-the-icy-moons-of-saturn doi: 10.2458/azu_uapress_9780816537075-ch003

Gorce, J., Caddick, M., & Bodnar, R. (2019, August). Thermodynamic constraints on carbonate stability and carbon volatility during subduction. *Earth and Planetary Science Letters*, *519*, 213–222. Retrieved from https://www.sciencedirect.com/science/article/pii/S0012821X19302596 doi: 10.1016/j.epsl.2019.04.047

Greeley, R., Chyba, C. F., Head, J., McCord, T., McKinnon, W. B., Pappalardo, R. T., ... others (2004). Geology of Europa. In *Jupiter: The Planet, Satellites and Magnetosphere* (pp. 329–362). (Publisher: Cambridge Univ. Press New York)

Hand, K., Carlson, R., & Chyba, C. (2007). Energy, chemical disequilibrium, and geological constraints on Europa. *Astrobiology*, *7*(6), 1006–1022.

Hansen, G. B., & McCord, T. B. (2008, January). Widespread CO2 and other non-ice compounds on the anti-Jovian and trailing sides of Europa from Galileo/NIMS observations. *Geophysical Research Letters*, *35*(1). Retrieved 2020-10-08, from https://doi.org/10.1029/2007GL031748 (Publisher: John Wiley & Sons, Ltd) doi: 10.1029/2007GL031748

Huss, G. R., Rubin, A. E., & Grossman, J. N. (2006). Thermal Metamorphism in Chondrites. In D. S. Lauretta & H. Y. McSween (Eds.), *Meteorites and the Early Solar System II* (pp. 567–586). Tucson, AZ: University of Arizona Press.

Hussmann, H., & Spohn, T. (2004). Thermal-orbital evolution of Io and Europa. *Icarus*, *171*(2), 391 - 410. Retrieved from http://www.sciencedirect.com/science/article/pii/S0019103504001952 doi: https://doi.org/10.1016/j.icarus.2004.05.020

Kalousová, K., & Sotin, C. (2020, September). Dynamics of Titan's high-pressure ice layer. *Earth and Planetary Science Letters*, *545*, 116416. Retrieved from http://www.sciencedirect.com/science/article/pii/S0012821X20303605 doi: 10.1016/j.epsl.2020.116416

Kargel, J. S. (1991, December). Brine volcanism and the interior structures of asteroids and icy satellites. *Icarus*, *94*(2), 368–390. Retrieved from http://www.sciencedirect.com/science/article/pii/001910359190235L doi: 10.1016/0019-1035(91)90235-L

Kargel, J. S., Kaye, J. Z., Head, J. W., Marion, G. M., Sassen, R., Crowley, J. K., ... Hogenboom, D. L. (2000). Europa's Crust and Ocean: Origin, Composition, and the Prospects for Life. *Icarus*, *148*(1), 226–265. Retrieved from http://www.sciencedirect.com/science/article/pii/S0019103500964716 doi: 10.1006/icar.2000.6471

Klimczak, C., Byrne, P. K., Regensburger, P. V., Bohnenstiehl, D. R., Hauck, S. A., II, Dombard, A. J., ... Elder, C. M. (2019, March). Strong Ocean Floors Within Europa, Titan, and Ganymede Limit Geological Activity There; Enceladus Less So. In (p. 2912). Retrieved from https://ui.adsabs.harvard.edu/abs/2019LPI....50.2912K

Kuramoto, K., & Matsui, T. (1994, October). Formation of a hot proto-atmosphere on the accreting giant icy satellite: Implications for the origin and evolution of Titan, Ganymede, and Callisto. *Journal of Geophysical Research: Planets*, *99*(E10), 21183–21200. Retrieved 2021-01-29, from

https://doi.org/10.1029/94JE01864 (Publisher: John Wiley & Sons, Ltd) doi: 10.1029/94JE01864

Kuskov, O., & Kronrod, V. (2005). Internal structure of Europa and Callisto. *Icarus*, *177*(2), 550 - 569. Retrieved from http://www.sciencedirect.com/science/article/pii/S0019103505001806 doi: https://doi.org/10.1016/j.icarus.2005.04.014

Leitner, M. A., & Lunine, J. I. (2019, November). Modeling early Titan's ocean composition. *Icarus*, *333*, 61–70. Retrieved 2020-07-08, from https://linkinghub.elsevier.com/retrieve/pii/S0019103518303312 doi: 10.1016/j.icarus.2019.05.008

Ligier, N., Poulet, F., Carter, J., Brunetto, R., & Gourgeot, F. (2016, may). VLT/SINFONI Observations of Europa: New insights into the surface composition. *The Astronomical Journal*, *151*(6), 163. Retrieved from https://doi.org/10.3847%2F0004-6256%2F151%2F6%2F163 doi: 10.3847/0004-6256/151/6/163

Lobo, A. H., Thompson, A. F., Vance, S. D., & Tharimena, S. (2021, April). A pole-to-equator ocean overturning circulation on Enceladus. *Nature Geoscience*, *14*(4), 185–189. Retrieved from https://doi.org/10.1038/s41561-021-00706-3 doi: 10.1038/s41561-021-00706-3

Lunine, J. I., & Nolan, M. C. (1992, November). A massive early atmosphere on Triton. *Icarus*, *100*(1), 221–234. Retrieved from http://www.sciencedirect.com/science/article/pii/0019103592900312 doi: 10.1016/0019-1035(92)90031-2

Lunine, J. I., & Stevenson, D. J. (1982, October). Formation of the galilean satellites in a gaseous nebula. *Icarus*, *52*(1), 14–39. Retrieved from https://www.sciencedirect.com/science/article/pii/001910358290166X doi: 10.1016/0019-1035(82)90166-X

Makalkin, A. B., Dorofeeva, V. A., & Ruskol, E. L. (1999, January). Modeling the Protosatellite Circum-Jovian Accretion Disk: An Estimate of the Basic Parameters. *Solar System Research*, *33*, 456.

Manthilake, G., Bolfan-Casanova, N., Novella, D., Mookherjee, M., & Andrault, D. (2016, May). Dehydration of chlorite explains anomalously high electrical conductivity in the mantle wedges. *Science Advances*, *2*(5), e1501631. Retrieved from http://advances.sciencemag.org/content/2/5/e1501631.abstract doi: 10.1126/sciadv.1501631

Marion, G. M., Kargel, J. S., Catling, D. C., & Jakubowski, S. D. (2005, January). Effects of pressure on aqueous chemical equilibria at subzero temperatures with applications to Europa. *Geochimica et Cosmochimica Acta*, *69*(2), 259–274. Retrieved 2018-09-30, from http://linkinghub.elsevier.com/retrieve/pii/S0016703704004880 doi: 10.1016/j.gca.2004.06.024

Marounina, N., & Rogers, L. A. (2020, February). Internal Structure and CO2 Reservoirs of Habitable Water Worlds. *The Astrophysical Journal*, *890*(2), 107. Retrieved from http://dx.doi.org/10.3847/1538-4357/ab68e4 (Publisher: American Astronomical Society) doi: 10.3847/1538-4357/ab68e4

Mayne, M. J., Moyen, J.-F., Stevens, G., & Kaislaniemi, L. (2016, May). Rcrust: a tool for calculating path-dependent open system processes and application to melt loss. *Journal of Metamorphic Geology*, *34*(7), 663–682. Retrieved 2018-07-25, from https://doi.org/10.1111/jmg.12199 doi: 10.1111/jmg.12199

McCord, T. B., Hansen, G. B., Fanale, F. P., Carlson, R. W., Matson, D. L., Johnson, T. V., ... Granahan, J. C. (1998, May). Salts on Europa's Surface Detected by Galileo's Near Infrared Mapping Spectrometer. *Science*, *280*(5367), 1242. Retrieved from http://science.sciencemag.org/content/280/5367/1242.abstract doi: 10.1126/science.280.5367.1242

McKinnon, W. B., & Zolensky, M. E. (2003). Sulfate Content of Europa's Ocean and Shell: Evolutionary Considerations and Some Geological and Astrobio-

logical Implications. *Astrobiology*, *3*(4), 879–897. Retrieved 2020-04-06, from https://doi.org/10.1089/153110703322736150 (Publisher: Mary Ann Liebert, Inc., publishers) doi: 10.1089/153110703322736150

Melwani Daswani, M. (2020, May). *AccretR*. Zenodo. Retrieved 2021-05-08, from https://zenodo.org/record/3827540 doi: 10.5281/ZENODO.3827540

Miller, K. E., Glein, C. R., & Waite, J. H. (2019, Jan). Contributions from accreted organics to Titan's atmosphere: New insights from cometary and chondritic data. *The Astrophysical Journal*, *871*(1), 59. Retrieved from http://dx.doi.org/10.3847/1538-4357/aaf561 doi: 10.3847/1538-4357/aaf561

Moore, W. B., & Hussmann, H. (2009). Thermal evolution of Europa's silicate interior. In R. T. Pappalardo, W. B. McKinnon, & K. Khurana (Eds.), *Europa* (pp. 369–380). Tucson: University of Arizona Press.

Mosqueira, I., Estrada, P., & Turrini, D. (2010, June). Planetesimals and Satellitesimals: Formation of the Satellite Systems. *Space Science Reviews*, *153*(1-4), 431–446. Retrieved 2021-04-13, from http://link.springer.com/10.1007/s11214-009-9614-6 doi: 10.1007/s11214-009-9614-6

Néri, A., Guyot, F., Reynard, B., & Sotin, C. (2020, Oct). A carbonaceous chondrite and cometary origin for icy moons of Jupiter and Saturn. *Earth and Planetary Science Letters*, 115920. Retrieved from http://dx.doi.org/10.1016/j.epsl.2019.115920 doi: 10.1016/j.epsl.2019.115920

Odert, P., Lammer, H., Erkaev, N., Nikolaou, A., Lichtenegger, H., Johnstone, C., ... Tosi, N. (2018, June). Escape and fractionation of volatiles and noble gases from Mars-sized planetary embryos and growing protoplanets. *Icarus*, *307*, 327–346. Retrieved from http://www.sciencedirect.com/science/article/pii/S0019103517301677 doi: 10.1016/j.icarus.2017.10.031

Pan, D., Spanu, L., Harrison, B., Sverjensky, D. A., & Galli, G. (2013, April). Dielectric properties of water under extreme conditions and transport of carbonates in the deep Earth. *Proceedings of the National Academy of Sciences*, *110*(17), 6646. Retrieved from http://www.pnas.org/content/110/17/6646.abstract doi: 10.1073/pnas.1221581110

Pasek, M. A., & Greenberg, R. (2012). Acidification of Europa's subsurface ocean as a consequence of oxidant delivery. *Astrobiology*, *12*(2), 151–159.

Reed, M. H. (1998). Calculation of simultaneous chemical equilibria in aqueous-mineral-gas systems and its application to modeling hydrothermal processes. In J. P. Richards (Ed.), *Techniques in Hydrothermal Ore Deposits Geology* (Vol. 10, pp. 109–124). Littleton, CO: Society of Economic Geologists, Inc.

Richard, G., Monnereau, M., & Rabinowicz, M. (2007, March). Slab dehydration and fluid migration at the base of the upper mantle: implications for deep earthquake mechanisms. *Geophysical Journal International*, *168*(3), 1291–1304. Retrieved 2020-06-27, from https://doi.org/10.1111/j.1365-246X.2006.03244.x doi: 10.1111/j.1365-246X.2006.03244.x

Ronnet, T., & Johansen, A. (2020, January). Formation of moon systems around giant planets: Capture and ablation of planetesimals as foundation for a pebble accretion scenario. *Astronomy & Astrophysics*, *633*, A93. Retrieved 2021-04-13, from https://www.aanda.org/10.1051/0004-6361/201936804 doi: 10.1051/0004-6361/201936804

Ronnet, T., Mousis, O., & Vernazza, P. (2017). Pebble Accretion at the Origin of Water in Europa. *The Astrophysical Journal*, *845*(2), 92. Retrieved 2018-12-18, from http://stacks.iop.org/0004-637X/845/i=2/a=92?key=crossref.e075ce27e4a38f6e8b1624cbb3608530 doi: 10.3847/1538-4357/aa80e6

Roth, L., Saur, J., Retherford, K. D., Strobel, D. F., Feldman, P. D., McGrath, M. A., & Nimmo, F. (2014, January). Transient Water Vapor at Europa's South Pole. *Science*, *343*(6167), 171. Retrieved from http://science.sciencemag.org/content/343/6167/171.abstract doi: 10.1126/science.1247051

Schubert, G., Sohl, F., & Hussmann, H. (2009). Interior of Europa. In R. T. Pappalardo, W. B. McKinnon, & K. Khurana (Eds.), *Europa* (pp. 353–367). Tucson: University of Arizona Press.

Sohl, F., Spohn, T., Breuer, D., & Nagel, K. (2002). Implications from galileo observations on the interior structure and chemistry of the galilean satellites. *Icarus*, *157*(1), 104 - 119. Retrieved from http://www.sciencedirect.com/science/article/pii/S0019103502968284 doi: https://doi.org/10.1006/icar.2002.6828

Sparks, W. B., Hand, K. P., McGrath, M. A., Bergeron, E., Cracraft, M., & Deustua, S. E. (2016, September). Probing for evidence of plumes on Europa with HST/STIS. *The Astrophysical Journal*, *829*(2), 121. Retrieved from http://dx.doi.org/10.3847/0004-637X/829/2/121 (Publisher: American Astronomical Society) doi: 10.3847/0004-637x/829/2/121

Tobie, G., Choblet, G., & Sotin, C. (2003). Tidally heated convection: Constraints on Europa's ice shell thickness. *Journal of Geophysical Research: Planets*, *108*(E11). Retrieved 2019-01-08, from https://doi.org/10.1029/2003JE002099 doi: 10.1029/2003JE002099

Tobie, G., Mocquet, A., & Sotin, C. (2005). Tidal dissipation within large icy satellites: Applications to Europa and Titan. *Europa Icy Shell*, *177*(2), 534–549. Retrieved from http://www.sciencedirect.com/science/article/pii/S0019103505001582 doi: 10.1016/j.icarus.2005.04.006

Townsend, M., & Huber, C. (2020, February). A critical magma chamber size for volcanic eruptions. *Geology*, *48*(5), 431–435. Retrieved 2020-05-20, from https://doi.org/10.1130/G47045.1 doi: 10.1130/G47045.1

Trumbo, S. K., Brown, M. E., Fischer, P. D., & Hand, K. P. (2017). A new spectral feature on the trailing hemisphere of Europa at 3.78 μm. *The Astronomical Journal*, *153*(6), 250. Retrieved from https://doi.org/10.3847%2F1538-3881%2Faa6d80 doi: 10.3847/1538-3881/aa6d80

Trumbo, S. K., Brown, M. E., & Hand, K. P. (2019). Sodium chloride on the surface of Europa. *Science Advances*, *5*(6). Retrieved from https://advances.sciencemag.org/content/5/6/eaaw7123 doi: 10.1126/sciadv.aaw7123

Vance, S. D., Hand, K. P., & Pappalardo, R. T. (2016, May). Geophysical controls of chemical disequilibria in Europa. *Geophysical Research Letters*, *43*(10), 4871–4879. Retrieved 2019-03-27, from https://doi.org/10.1002/2016GL068547 doi: 10.1002/2016GL068547

Vance, S. D., Panning, M. P., Stähler, S., Cammarano, F., Bills, B. G., Tobie, G., ... Banerdt, B. (2018). Geophysical investigations of habitability in ice-covered ocean worlds. *Journal of Geophysical Research: Planets*, *123*(1), 180-205. Retrieved from https://agupubs.onlinelibrary.wiley.com/doi/abs/10.1002/2017JE005341 doi: 10.1002/2017JE005341

Vance, S. D., Styczinski, M., Melwani Daswani, M., & Vega, K. (2020, September). *vancesteven/PlanetProfile: Supplementary Data: Magnetic Induction Responses of Jupiter's Ocean Moons Including Effects from Adiabatic Convection.* Zenodo. Retrieved 2021-05-08, from https://zenodo.org/record/4052711 doi: 10.5281/ZENODO.4052711

Wakita, S., & Genda, H. (2019, August). Fates of hydrous materials during planetesimal collisions. *Icarus*, *328*, 58–68. Retrieved from http://www.sciencedirect.com/science/article/pii/S0019103518306523 doi: 10.1016/j.icarus.2019.03.008

Zahnle, K. J., & Catling, D. C. (2017, July). The Cosmic Shoreline: The Evidence that Escape Determines which Planets Have Atmospheres, and what this May Mean for Proxima Centauri B. *The Astrophysical Journal*, *843*(2), 122. Retrieved from http://dx.doi.org/10.3847/1538-4357/aa7846 (Publisher: American Astronomical Society) doi: 10.3847/1538-4357/aa7846

Zolotov, M. Y., & Kargel, J. S. (2009). On the chemical composition of Europa's icy

shell, ocean, and underlying rocks. In R. T. Pappalardo, W. B. McKinnon, & K. Khurana (Eds.), *Europa* (p. 431). University of Arizona Press Tucson, AZ. Retrieved from https://uapress.arizona.edu/book/europa

Zolotov, M. Y., & Shock, E. L. (2001). Composition and stability of salts on the surface of Europa and their oceanic origin. *Journal of Geophysical Research: Planets*, *106*(E12), 32815–32827. Retrieved 2018-10-19, from https://doi.org/10.1029/2000JE001413 doi: 10.1029/2000JE001413

Zolotov, M. Y., & Shock, E. L. (2004). A model for low-temperature biogeochemistry of sulfur, carbon, and iron on Europa. *Journal of Geophysical Research: Planets*, *109*(E6). Retrieved 2018-10-19, from https://doi.org/10.1029/2003JE002194 doi: 10.1029/2003JE002194

Figure 1.

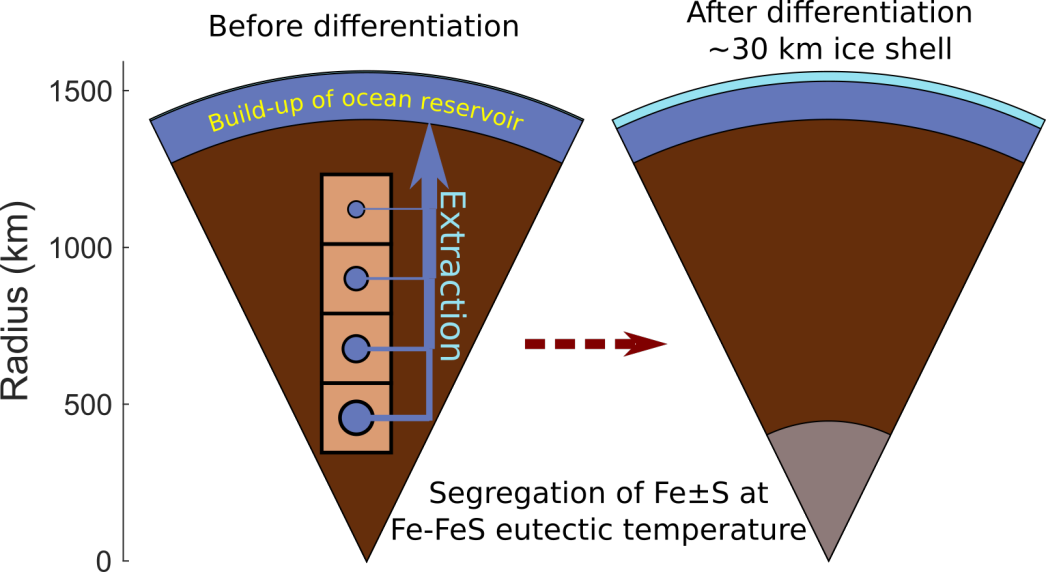
Before differentiation
After differentiation
~30 km ice shell
Build-up of ocean reservoir
Extraction
Radius (km)
1500
1000
500
0
Segregation of Fe±S at
Fe-FeS eutectic temperature

Figure 2.

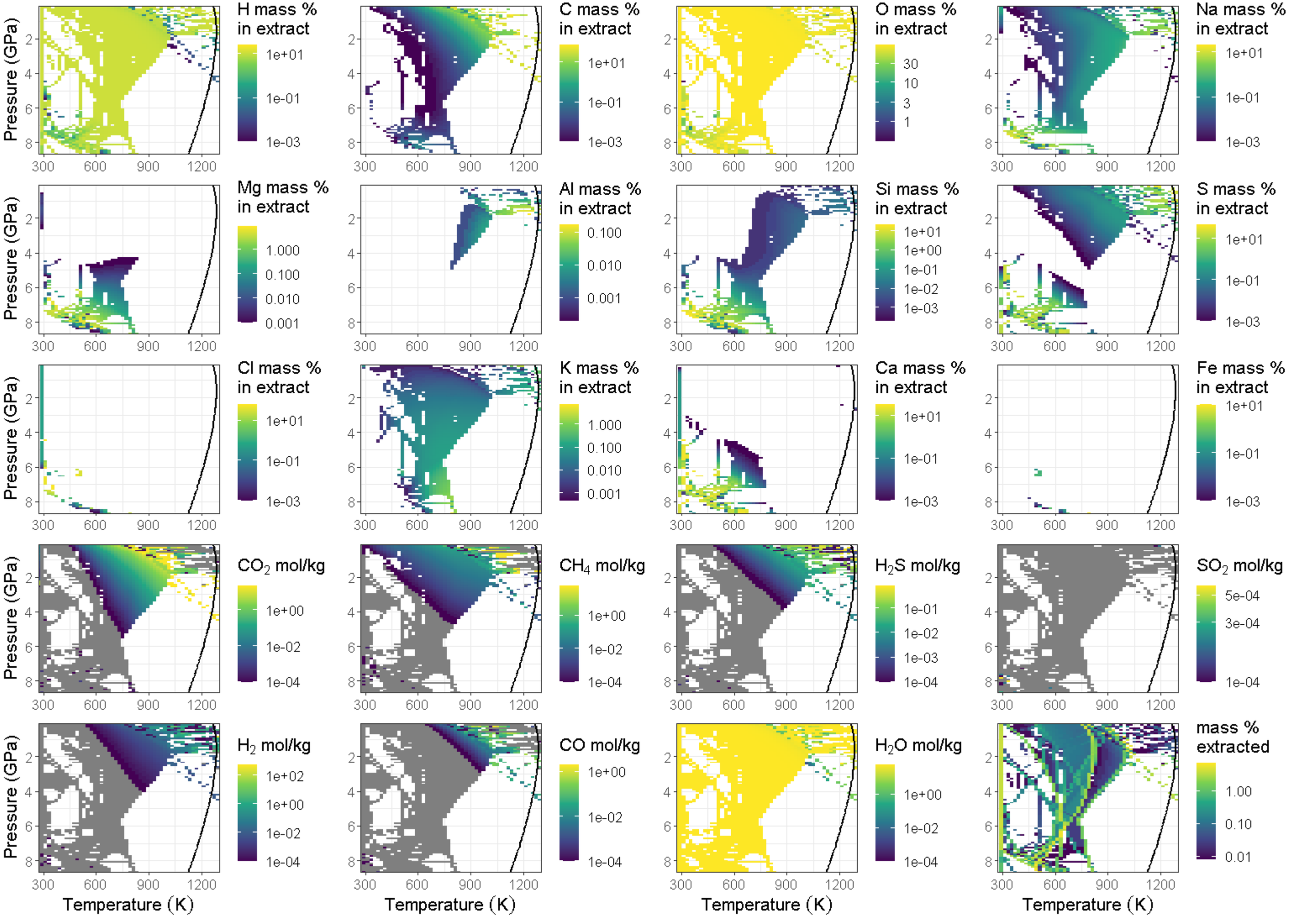
H mass % in extract
1e+01
1e-01
1e-03
C mass % in extract
1e+01
1e-01
1e-03
O mass % in extract
30
10
3
1
Na mass % in extract
1e+01
1e-01
1e-03
Mg mass % in extract
1.000
0.100
0.010
0.001
Al mass % in extract
0.100
0.010
0.001
Si mass % in extract
1e+01
1e+00
1e-01
1e-02
1e-03
S mass % in extract
1e+01
1e-01
1e-03
Cl mass % in extract
1e+01
1e-01
1e-03
K mass % in extract
1.000
0.100
0.010
0.001
Ca mass % in extract
1e+01
1e-01
1e-03
Fe mass % in extract
1e+01
1e-01
1e-03
CO2 mol/kg
1e+00
1e-02
1e-04
CH4 mol/kg
1e+00
1e-02
1e-04
H2S mol/kg
1e-01
1e-02
1e-03
1e-04
SO2 mol/kg
5e-04
3e-04
1e-04
H2 mol/kg
1e+02
1e+00
1e-02
1e-04
CO mol/kg
1e+00
1e-02
1e-04
H2O mol/kg
1e+00
1e-02
1e-04
mass % extracted
1.00
0.10
0.01
Pressure (GPa)
Temperature (K)
300
600
900
1200
2
4
6
8

Figure 3.

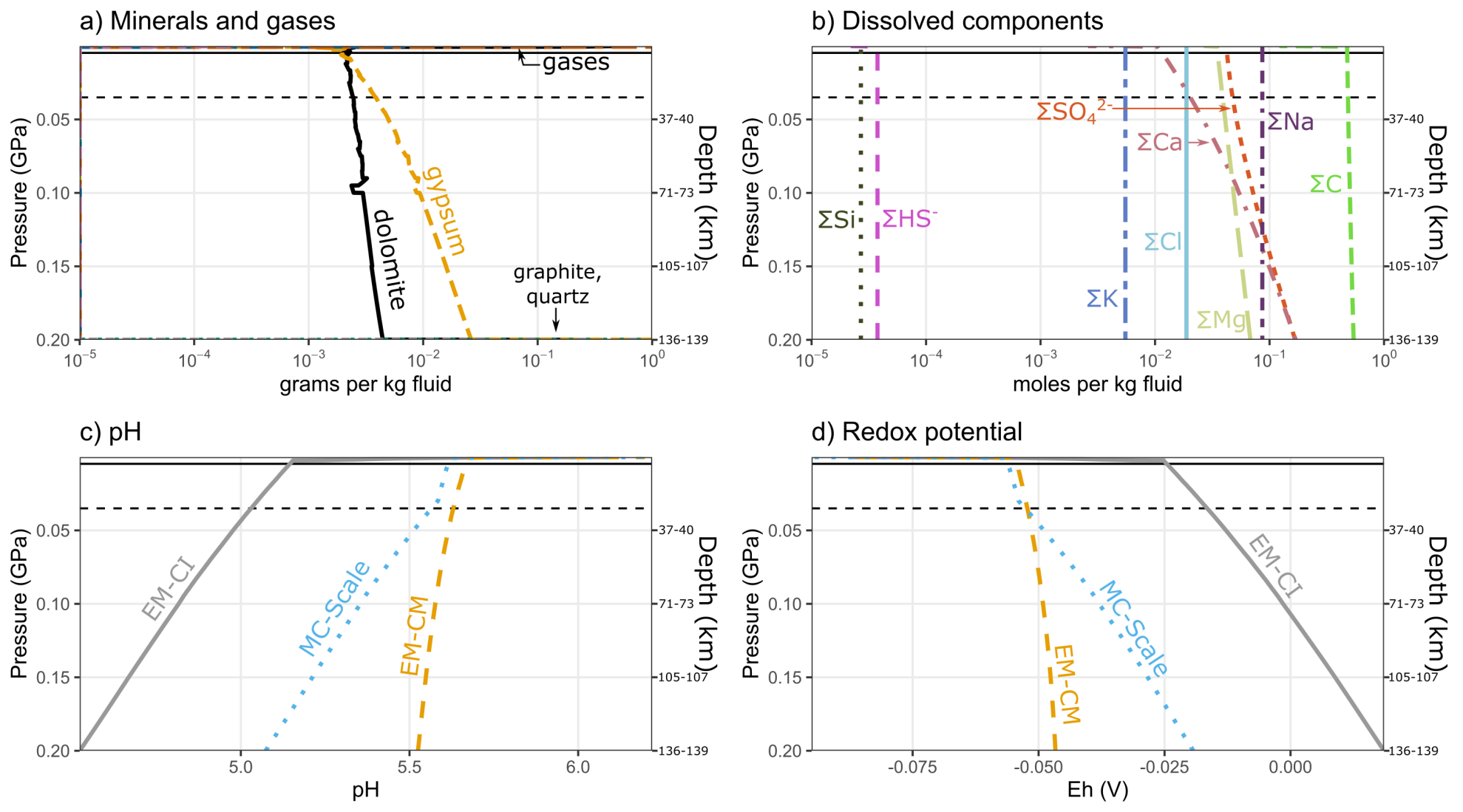
a) Minerals and gases
gases
gypsum
dolomite
graphite,
quartz
Pressure (GPa)
Depth (km)
grams per kg fluid
b) Dissolved components
ΣSO4 2-
ΣNa
ΣCa
ΣC
ΣSi
ΣHS-
ΣCl
ΣK
ΣMg
moles per kg fluid
c) pH
EM-CI
MC-Scale
EM-CM
pH
d) Redox potential
Eh (V)